Effects of nonlocal potentials on (p,d) transfer reactions

A. Ross,[1,2] L. J. Titus,[1,2] F. M. Nunes,[1,2] M. H. Mahzoon,[3] W. H. Dickhoff,[3] and R. J. Charity[4]
[1]*National Superconducting Cyclotron Laboratory, Michigan State University, East Lansing, Michigan 48824, USA*
[2]*Department of Physics and Astronomy, Michigan State University, East Lansing, Michigan 48824-1321*
[3]*Department of Physics, Washington University, Saint Louis, Missouri 63130, USA*
[4]*Department of Chemistry, Washington University, Saint Louis, Missouri 63130, USA*
(Received 21 May 2015; revised manuscript received 21 September 2015; published 15 October 2015)

Background: Although local phenomenological optical potentials have been standardly used to interpret nuclear reactions, recent studies suggest the effects of nonlocality should not be neglected.

Purpose: In this work we investigate the effects of nonlocality in (p,d) transfer reactions using nonlocal optical potentials. We compare results obtained with the dispersive optical model to those obtained using the Perey-Buck interaction.

Method: We solve the scattering and bound-state equations for the nonlocal version of the dispersive optical model. Then, using the distorted-wave Born approximation, we calculate the transfer cross section for (p,d) on ^{40}Ca at $E_p = 20$, 35, and 50 MeV.

Results: The inclusion of nonlocality in the bound state has a larger effect than that in the scattering states. The overall effect on the transfer cross section is very significant. We found an increase due to nonlocality in the transfer cross section of ≈30–50% when using the Perey-Buck interaction and of ≈15–50% when using the dispersive optical potential.

Conclusions: Although the details of the nonlocal interaction can change the magnitude of the effects, our study shows that qualitatively the results obtained using the dispersive optical potential and the Perey-Buck interaction are consistent, in both cases the transfer cross sections are significantly increased.

DOI: 10.1103/PhysRevC.92.044607 PACS number(s): 21.10.Jx, 21.10.Pc, 24.10.Ht, 25.45.Hi

I. INTRODUCTION

Nuclear reactions offer an exceptional opportunity to probe the properties of nuclei away from stability. Of particular interest are single-nucleon transfer reactions involving deuterons. A number of experimental programs have focused on measuring (d,p) or (p,d) reactions with the motivation of learning about shell evolution and the configuration of the valence nucleons in exotic nuclei (e.g., Refs. [1,2]). These types of reactions are also used to extract astrophysical information and quantities relevant to stockpile stewardship (e.g., Refs. [3–5]). From a theoretical perspective, these reactions are attractive because they can be reduced to a three-body problem composed of $n + p + A$.

In recent years, there have been many efforts to improve the description of $(d,p)/(p,d)$ transfer reactions. Studies benchmarking various methods have exposed serious limitations in even the most advanced approaches [6–9]. Although the methodology for accurately solving the three-body scattering problem is under intense research, there are at least two less-tractable sources of uncertainty in the calculation of transfer reaction observables, namely, the reduction of the many-body problem to a three-body problem and the uncertainties in the effective interactions introduced as a consequence of that reduction [10]. The context of this work is associated with the second aspect, namely, the uncertainties in the so-called optical potentials.

Traditionally, nucleon optical potentials have been derived phenomenologically, primarily from fitting elastic-scattering data but sometimes the fits also include total and absorption cross sections and polarization observables (e.g., Refs. [11–14]). The common assumption in all of these global optical-model fits is that the interaction is made local, and to compensate for this, a strong energy dependence of the potential is introduced. From a microscopic standpoint, the effective interaction between the nucleons is inherently nonlocal and one expects that the nonlocality is mostly felt in the nuclear interior. Perey and Buck [15] developed a nonlocal global potential in the sixties using a standard real volume Woods-Saxon form and an imaginary surface term for the optical potential, multiplied by a single Gaussian nonlocality with a range of 0.85 fm. With this potential, they showed that the elastic-scattering data for a variety of nuclei ranging from light to heavy masses could be reproduced without introducing explicit energy dependence in the optical-model parameters.

Motivated by earlier work [7], we recently performed a systematic study of the effects of nonlocality in the nucleon-nucleus effective interactions in (p,d) transfer reactions used for studying single-particle states [16]. All calculations in Ref. [16] were based on the Perey-Buck (PB) optical potential and compared with local phase equivalents obtained for this interaction. Consistent with what had been found before [17,18], we found that nonlocality affects the scattering wave functions in the nuclear interior out to the surface region. Nonlocality similarly affects the bound state in the nuclear interior, but also beyond the surface region because it changes the asymptotic normalization coefficient. When introducing the wave functions obtained with nonlocal interactions in the transfer matrix element, we obtained very significant differences compared to those obtained with the phase-equivalent interactions. Typically the nonlocality in the bound state increased the cross section, while nonlocality in

the scattering state decreased it. Although we found some cancellation when putting both effects together, the overall effect was still found to be very significant, of the order of an ≈10–30% change in the differential cross section at the peak of the angular distribution. A standard way to take care of the nonlocal effects on the wave function, without solving a nonlocal equation, is through the introduction of the so-called Perey factor [17,18]. As shown in Ref. [16], this factor does not provide an accurate description of nonlocality in transfer reactions. Given that the study of Ref. [16] focused exclusively on the PB interaction, which has a rather simple form, it was unclear to us whether these results could be generalized.

An alternative method for obtaining the optical potential was introduced by Mahaux and Sartor [19], which included the use of dispersion relations. One of the main attractions of the dispersive optical model (DOM) is that it connects bound-state properties (the real part of the self-energy at the Fermi energy) and scattering (the imaginary part of the optical potential) through a dispersion relation [20]. The local DOM optical potential developed in Ref. [20] was used in (d,p) transfer reactions on closed-shell nuclei, and results demonstrate that the DOM potentials are able to describe the transfer angular distributions at least as well as other global phenomenological optical potentials on the market [21]. Because the local version of the DOM still contains an energy dependence related to nonlocality of the real part, it distorts the normalization of the spectral strength and requires a correction for the proper normalization of spectroscopic factors. A nonlocal Hartree-Fock-like and energy-independent potential was introduced in Ref. [22] to avoid this issue. While this step allowed the interpretation of the optical potential as representing the nucleon self-energy, it was also shown that observables like the nuclear charge density cannot be described in detail. By analyzing theoretically calculated self-energies for Ca isotopes which include long-range [23] and short-range correlations [24], it was possible to clarify the importance of representing the imaginary part of the optical potential also in terms of nonlocal ingredients. These insights have recently led to an extension of the DOM formalism to explicitly include nonlocality [25,26] in the real and imaginary parts of the self-energy specifically for the ^{40}Ca nucleus. To fit a large range of bound-state and scattering data, the nonlocality was required to be different above and below the Fermi energy for the imaginary components. In addition the real potential required a more complicated nonlocality than the standard Gaussian form. The final result includes an accurate representation of the nuclear charge density, spectral information including high-momentum nucleons obtained from $(e,e'p)$ data [27] in addition to all elastic-scattering data up to 200 MeV. Note that because the Perey factor [17] was derived explicitly for a potential with the simple form of the PB interaction, it cannot be easily generalized to the DOM case. For this reason, the Perey factor study included in Ref. [16] is not part of the present study.

In this work, we revisit the study in Ref. [16], but now using the DOM nonlocal interaction of Ref. [25] for the reactions ^{40}Ca$(p,d)^{39}$Ca at $E_p = 20$, 35, and 50 MeV. For comparison, we also repeat the calculations with the PB interaction for these reactions. In Sec. II, we provide details of the numerical inputs. In Sec. III we present the results, and finally in Sec. IV we draw our conclusions.

II. NUMERICAL INPUTS

To understand the role of nonlocality in transfer reactions, it is critical to have a local phase-equivalent (PE) interaction. Thus, the first step in our work was to fit in detail the elastic-scattering predictions obtained with both the DOM [25] and the PB [15] nonlocal interactions, with a local form. So far, the nonlocal DOM has only been developed for ^{40}Ca, so we concentrated our investigation to proton scattering on ^{40}Ca at $E_p = 20$, 35, and 50 MeV.

To mimic the complex shape of the nonlocal DOM interaction introduced in Ref. [25], its PE potential was chosen to include, in the real part, two volume terms of Woods-Saxon form and a spin-orbit force. The imaginary part contains a volume term, of Woods-Saxon form, a surface term proportional to the derivative of a Woods-Saxon form, and a spin-orbit term. The Coulomb potential was generated from a homogeneous charged sphere of radius $R = 1.22A^{1/3}$. The final PE form used in the fit to the nonlocal DOM elastic-scattering predictions is

$$\begin{aligned} U^{\text{DOM-PE}}(R) = & -V_{\text{vol1}} f(R,r_{\text{vol1}},a_{\text{vol1}}) \\ & - V_{\text{vol2}} f(R,r_{\text{vol2}},a_{\text{vol2}}) - i W_{\text{vol}} f\left(R,r_w^{\text{vol}},a_w^{vol}\right) \\ & + i4a_{\text{surf}} W_{\text{surf}} \frac{d}{dR} f\left(R,r_w^{\text{surf}},a_w^{\text{surf}}\right) \\ & + V^{\text{so}}(R) + V_C(R) + i W^{\text{so}}(R), \end{aligned} \quad (1)$$

where

$$f(R,r,a) = \left[1 + \exp\left(\frac{R - rA^{1/3}}{a}\right)\right]^{-1} \quad (2)$$

and A is the mass number of the target. The parameters obtained from the fit to the predicted DOM elastic-scattering angular distributions are presented in Table I.

The PB nonlocal interaction contains only one real volume term and an imaginary surface term, multiplied by a Gaussian nonlocality [15]. We keep this simple shape in the parametrization of its local phase equivalent:

$$\begin{aligned} U^{\text{PB-PE}}(R) = & -V_{\text{vol}} f(R,r_{\text{vol}},a_{\text{vol}}) + i4a_{\text{surf}} W_{\text{surf}} \frac{d}{dR} \\ & \times f(R,r_{\text{surf}},a_{\text{surf}}) + V_C(R) + V^{\text{so}}(R), \end{aligned} \quad (3)$$

where we have used the same Coulomb parameters as in Ref. [15]. The fitted parameters obtained with this interaction are presented in Table II.

For illustration purposes, we show in Figs. 1 and 2 the elastic-scattering angular distributions obtained for $p + ^{40}$Ca at proton energies of $E_p = 20$ and 50 MeV, normalized to Rutherford. Experimental results are indicated by the diamond-shaped data points, predictions with the nonlocal interactions (solid line for the DOM and dashed line for PB) can be compared to their corresponding local PEs (open circles for the results with the DOM local PE and open squares for the results with the PB local PE). The angular distribution for the DOM PE agrees well with the predictions obtained with

TABLE I. DOM PE potential parameters corresponding to the various proton beam energies considered.

	20 MeV	35 MeV	50 MeV
$V_{\rm vol1}$	14.556	19.817	8.885
$r_{\rm vol1}$	1.242	1.300	1.299
$a_{\rm vol1}$	0.601	0.680	0.680
$V_{\rm vol2}$	31.176	23.797	31.946
$r_{\rm vol2}$	1.272	1.100	1.101
$a_{\rm vol2}$	0.652	0.680	0.680
$W_{\rm vol}$	0.717	5.660	6.195
$r_w^{\rm vol}$	1.293	1.300	1.299
$a_w^{\rm vol}$	0.680	0.680	0.680
$W_w^{\rm surf}$	5.950	2.952	2.573
$r_w^{\rm surf}$	1.197	1.239	1.259
$a_w^{\rm surf}$	0.536	0.550	0.539
$V_{\rm so}$	3.773	1.908	3.469
$r_{\rm so}$	1.167	1.100	1.100
$a_{\rm so}$	0.615	0.600	0.602
$W_w^{\rm so}$	0.322	1.688	0.647
$r_w^{\rm so}$	1.220	1.100	1.299
$a_w^{\rm so}$	0.647	0.600	0.680

the nonlocal DOM. The same is true for the PB interaction. The PB interaction was not fit to Ca isotopes at all and therefore one does not expect it to follow the data closely. Conversely, the DOM potential was fit using a wide array of scattering data for neutrons and protons on ^{40}Ca, as well as bound-state properties. It is thus understandable that the elastic scattering predicted by the DOM and PB potentials differ, thus the importance of determining the local PE interaction for each case separately to isolate those effects coming only from nonlocality.

Because we are interested in transfer reactions populating a neutron bound state, we also need to consider nonlocality in the calculation of the bound-state wave function. For the particular reactions we are considering, this consists of a $1d_{3/2}$ bound state for $n + {}^{39}$Ca. The DOM predicts the shape of the mean field around the Fermi level. Therefore, we computed the bound-state wave function using the nonlocal DOM interaction obtained at the experimental bound-state energy of $E = -15.6$ MeV. The PB potential was only developed for scattering states; so following Ref. [16], the real part of the PB

TABLE II. Same as in Table I, but for the PE PB potential.

	20 MeV	35 MeV	50 MeV
$V_{\rm vol}$	44.224	40.708	37.449
$r_{\rm vol}$	1.298	1.286	1.267
$a_{\rm vol}$	0.614	0.617	0.610
$W_{\rm surf}$	10.181	9.542	8.917
$r_{\rm surf}$	1.250	1.248	1.236
$a_{\rm surf}$	0.423	0.420	0.420
$V_{\rm so}$	5.647	6.216	6.381
$r_{\rm so}$	1.255	1.248	1.258
$a_{\rm so}$	0.652	0.652	0.657

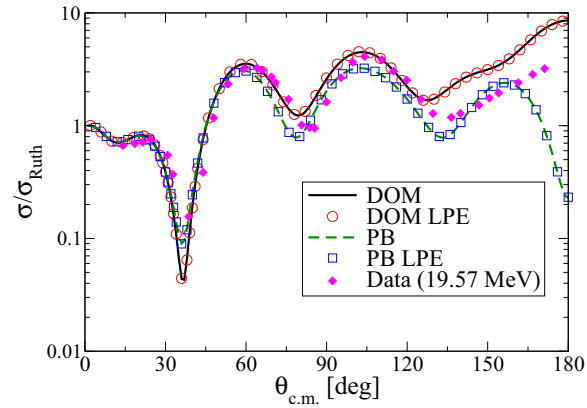

FIG. 1. (Color online) Angular distributions for elastic scattering normalized to Rutherford of protons on ^{40}Ca at $E_p = 20.0$ MeV. Predicted results with the nonlocal DOM potential (solid line), the DOM local PE (open circles), the PB interaction (dashed line), and the PB local PE (open squares) are compared to the experimental data (closed diamonds) of Ref. [28].

interaction was taken to produce the mean field for the bound state, assuming that around the Fermi level the imaginary part is zero. The overall strength of this mean field was then adjusted to reproduce the experimental binding energy of the system of interest. We also added a spin-orbit force with a standard strength of $V_{\rm so} = 6$ MeV.

The bound-state wave functions with these two nonlocal interactions are then compared with those obtained from the typical approach in our field, consisting of a single-particle state generated by a local mean field of Woods-Saxon form, with standard geometry (radius parameter $r = 1.25$ fm and diffuseness $a = 0.65$ fm) and a spin-orbit potential with strength of $V_{\rm so} = 6$ MeV. The depth of the Woods-Saxon interaction is adjusted to reproduce the experimental separation energy of $S_n = 15.6$ MeV.

The method used to solve the nonlocal Schrödinger equation for both scattering and bound states is described in detail in Ref. [16]. To study (p,d) transfer, we still need to define the V_{np} interaction that determines the deuteron ground-state wave

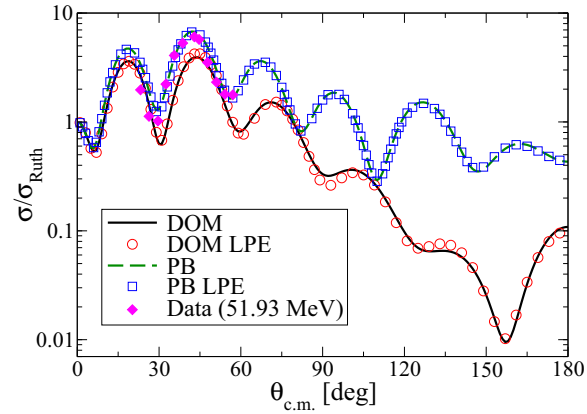

FIG. 2. (Color online) Same as for Fig. 1, but now for $E_p = 50$ MeV and the experimental data from Ref. [29].

function as well as the optical potential for the deuteron exit channel. We use the Reid interaction for the deuteron [30] and the Daenick global optical potential for $d + {}^{39}$Ca [31]. We then use the code FRESCO [32] to compute the transfer cross sections in the postform distorted-wave Born approximation (DWBA). Note that in general, the postform DWBA requires an auxiliary potential to be introduced, which distorts the proton in the final state and contributes to the remnant term in the operator of the corresponding T matrix. Traditionally, this potential is chosen to be the phenomenological potential that reproduces proton elastic scattering in the final state. For intermediate mass to heavy nuclei, this most often ensures that the remnant contribution is very small.

III. RESULTS

A. Nonlocal effects on the wave functions

Before considering transfer cross sections, we first investigate the effect of nonlocality on the wave functions themselves. In Fig. 3, we show the $p + {}^{40}$Ca scattering wave function for the $\ell = 0$ partial wave obtained by solving the nonlocal Schrödinger equation for both the DOM and the PB interactions at $E_p = 50$ MeV. These are compared with the wave functions obtained when using their respective PE interactions. This is one of the cases where the largest differences are observed. The main effect of nonlocality is to reduce the amplitude of the wave function in the nuclear interior. This is consistent with earlier studies [16–18].

The neutron $1d_{3/2}$ bound-state wave function is depicted in Fig. 4. As can be seen, the effect of nonlocality not only reduces the strength in the nuclear interior but also shifts the wave function out to larger radii, which results in a larger asymptotic normalization coefficient. Again this is consistent with results of Refs. [16,21]. When both mean fields are adjusted to reproduce the experimental binding energy, we see

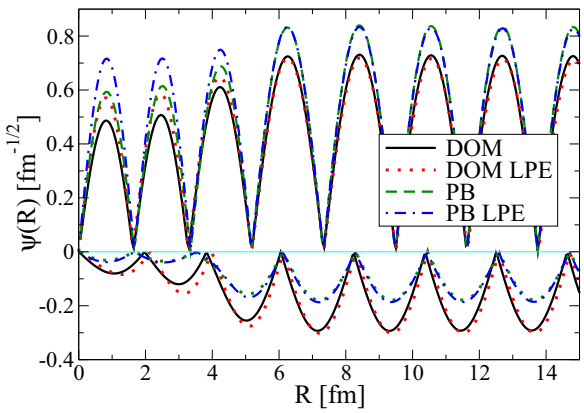

FIG. 3. (Color online) The real and imaginary parts of the $J^\pi = 1/2^+$ partial wave of the scattering wave function for the reaction ^{40}Ca$(p,p)^{40}$Ca at $E_p = 50.0$ MeV. This figure compares results obtained with the nonlocal DOM (solid line) and its local PE (dotted line), with the PB interaction (dashed line) and its local PE (dot-dashed line). The top (bottom) panel shows the absolute values of the real (imaginary) part of the scattering wave function. The coordinate R represents the relative distance $p - {}^{40}$Ca.

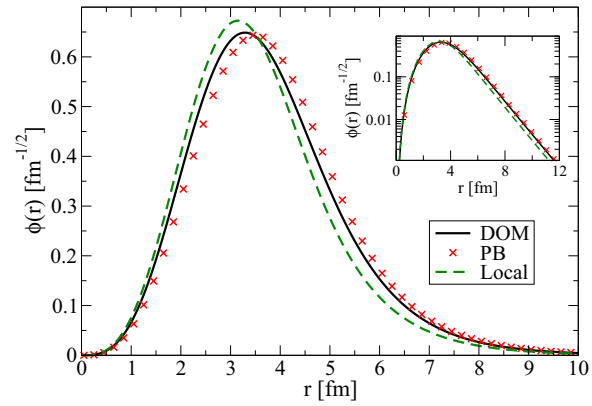

FIG. 4. (Color online) The neutron ground-state, $1d_{3/2}$, bound-state wave function for $n + {}^{39}$Ca. This figure compares the wave functions obtained with the DOM potential (solid line) to those obtained with the PB interaction (crosses) and the local interaction (dashed line). The coordinate r represents the relative distance $n - {}^{39}$Ca. The inset is the same figure in a log plot.

only minor differences between the bound-state wave function obtained using the PB and the DOM interactions. Futhermore, to quantify the effects of nonlocality in the bound state, we adjust the parameters of the Woods-Saxon form to mimic the wave function obtained by the nonlocal DOM potential. We are able to reproduce the DOM wave function with an increased radius and diffuseness ($r = 1.31$ fm and $a = 0.8$ fm) while preserving the same binding energy $S_n = 15.6$ MeV and the same asymptotic normalization. This quantifies what is intuitively seen in Fig. 4.

B. Transfer cross sections

We now turn our attention to the transfer cross sections obtained in the DWBA. In Fig. 5 we present the transfer angular distributions for the ^{40}Ca$(p,d)^{39}$Ca(g.s.) reaction at $E_p = 20$, 35, and 50 MeV. In this figure, we show the results of including nonlocality in both the proton incoming wave function and the initial neutron bound state, either with the DOM potential (solid lines) or with the PB interaction (dashed line). We compare these with the results obtained with local interactions: the DOM local PE (dotted line) and the PB local PE (dot-dashed line). Whether we consider the DOM or the PB potential, nonlocality affects not only the magnitude of the angular distribution but also the shape around the peak region typically used to extract structure information. These effects are consistent with those found in Ref. [16].

To quantify the effects of nonlocality in the potentials on the transfer reaction, we compare total cross sections as well as differential cross sections at the peak of the angular distribution. The first gives us an overall measure of the effect, integrating out shape differences, particularly at forward angles. The second is relevant when using transfer reactions to extract spectroscopic factors because only forward angles are used (as done in, e.g., Refs. [1,2]). In Table III we show the total cross sections obtained for the transfer process at three different beam energies, $E_p = 20$, 35, and 50 MeV, for the nonlocal and local equivalent DOM and PB potentials.

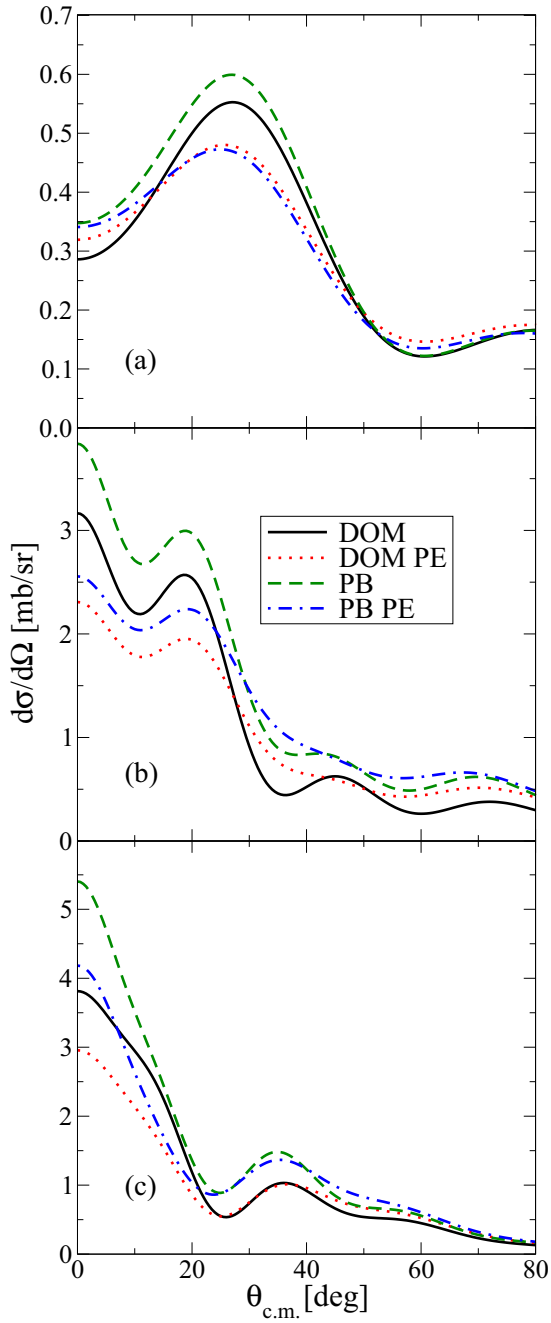

FIG. 5. (Color online) Angular distributions for the ^{40}Ca$(p,d)^{39}$Ca reaction at (a) $E_p = 20$ MeV, (b) $E_p = 35$ MeV, and (c) $E_p = 50$ MeV. This figure compares results obtained with the nonlocal DOM (solid line), the DOM local PE (dotted line), the PB interactions (dashed line), and the PB local PE (dot-dashed line).

Also shown are the percentage differences of nonlocal to local relative to local cross sections. Results show that for the DOM, it is only at the intermediate energy that nonlocality plays a role, and even in this case effects are not very large. For the PB potential, the effect of nonlocality is only significant at 20 MeV.

We then look at the percentage difference of the differential cross sections at the peak of the angular distribution relative to those resulting from local interactions only. The percentage differences are listed in Tables IV and V for the DOM and PB potentials, respectively, at the three different beam energies considered: $E_p = 20$, 35, and 50 MeV. We show the separate effects of nonlocality in the neutron bound state and the proton-scattering state. To do this, we repeat the calculations for the ^{40}Ca$(p,d)^{39}$Ca transfer reaction including only nonlocality in the calculation of either the bound state or the scattering state. The effect of nonlocality in the bound state at all proton energies considered is to increase the magnitude of the transfer cross section. This large effect is caused by the shift of the bound-state wave function towards the nuclear periphery. The T matrix for these reactions is mostly sensitive to the peripheral region and therefore picks up that additional strength. The effect of nonlocality in the scattering state is not as pronounced as for the bound state, reducing the transfer cross section in most cases. The total effect is shown in the last column of Tables IV and V and is very significant in all cases.

We note that the nonlocal effects shown here for the PB interaction are generally larger than those found in Ref. [16]. While in Ref. [16] we studied particle states in closed-shell nuclei, here we focus on a hole state in ^{40}Ca, which is much more deeply bound.

The percentage difference between the transfer cross sections obtained with nonlocal versus local interactions can vary considerably with beam energy. One naively expects that as the beam energy increases, the reaction will become less peripheral and therefore the strong enhancement felt from the asymptotic behavior of the bound-state wave function will become less pronounced. However, the calculations in this work appear to show no simple trend. A full DWBA calculation contains the remnant term corresponding to, in our case, the difference between the optical potential between the proton

TABLE III. Total ^{40}Ca$(p,d)^{39}$Ca(g.s.) cross sections at the listed beam energies using the DOM and PB potential relative to the calculations with their PE potentials. Also shown are the percentage difference between nonlocal and local cross sections. Total cross sections are given in mb.

E_p (MeV)	DOM	DOM-PE	% diff	PB	PB-PE	% diff
20	1.95	1.93	1.02	2.02	1.80	12.29
35	4.63	5.35	−13.46	6.51	6.42	1.28
50	3.55	3.62	−1.84	4.61	4.50	2.37

TABLE IV. Percent differences of the (p,d) transfer cross sections at the first peak at the listed beam energies using the DOM potential relative to the calculations with the phase-equivalent potential. Results are listed separately for the effects of nonlocality on the bound state, the scattering state, and the total.

E_p (MeV)	Bound state	Scattering state	Full nonlocal
20	27%	–14%	15%
35	31%	10%	52%
50	31%	–3%	29%

TABLE V. The same as for Table IV, but now for the PB potential.

E_p (MeV)	Bound state	Scattering state	Full nonlocal
20	42%	–15%	27%
35	55%	−8%	52%
50	42%	–11%	29%

and ^{39}Ca and the final proton ^{40}Ca optical potential. We have checked that for both energies this term is negligible.

IV. CONCLUSIONS

In this work we studied the effects of nonlocality in transfer reactions using a nonlocal potential obtained from the dispersive optical model [25] and comparing it to the results from the older PB interaction [15]. Our studies focused on the ^{40}Ca$(p,d)^{39}$Ca reaction at $E_p = 20$, 35, and 50 MeV. We considered the nonlocality in the proton channel and solved the integral-differential equation to obtain the proton scattering and neutron bound-state solutions for both nonlocal potentials. We then computed the transfer matrix element in the DWBA, ignoring nonlocality in the deuteron channel. To isolate the effects arising from nonlocality alone, we generated two local PE interactions that reproduced the elastic-scattering predictions from the nonlocal DOM and the PB potentials separately.

Our results show that, irrespective of the details of the potential, nonlocality reduces the strength of the wave function in the nuclear interior, an effect most noticeable in the bound states, but also significant in scattering states. Due to the normalization condition, nonlocality in the bound state also shifts the wave function to the periphery region, causing an increase in the forward-angle transfer cross sections. When nonlocality is considered only in the bound state, both DOM and PB potentials produce very large increases in the magnitude of the transfer cross sections (≈30–50%). Typically, nonlocality in the scattering state acts in the opposite direction, reducing the overall effect. When nonlocality is included in both the bound and the scattering states, the transfer differential cross sections are increased by ≈15–50% for the DOM potential, in contrast with ≈30–50% obtained with the PB interaction. In addition to this change in magnitude, nonlocality also changes the shape of the transfer angular distribution, an effect that may help to constrain the details of the nonlocal parameters. Finally, although qualitatively we find similar effects for all beam energies, there are significant quantitative variations in the magnitude of the differential cross section at the peak of the distribution, the largest effects being found for the intermediate energy of $E_p = 35$ MeV. The effects of nonlocality on the total cross sections are not important for either the DOM or the PB interactions.

In this study we focus on reactions on ^{40}Ca nuclei, because the nonlocal DOM was originally developed for this system. Meanwhile extensions of this optical potential to heavier Ca isotopes, as well as Sn and Pb, are under way. It will be interesting to perform a more systematic study across the nuclear chart to generalize our findings to other systems.

While in this work the transfer cross sections were calculated within the DWBA, it is understood that deuteron breakup should be included explicitly in the description of these transfer reactions (e.g., Ref. [1]). An effective method to include deuteron breakup is the finite-range adiabatic wave approximation but the exact treatment of nonlocality is intricate [33,34]. Work along these lines is now in the pipeline.

ACKNOWLEDGMENTS

We are grateful to Ron Johnson for useful discussions. This work was supported by the National Science Foundation, Directorate for Mathematical and Physical Science under Grants No. PHY-0800026 and No. PHY-1304242 and the U.S. Department of Energy, Office of Science, Office of Nuclear Physics, under Grants No. DE-FG52-08NA28552, No. DE-SC0004087, and No. DE-87ER-40316.

[1] K. Schmitt, K. Jones, A. Bey, S. Ahn, D. Bardayan *et al.*, Phys. Rev. Lett. **108**, 192701 (2012).
[2] K. L. Jones, F. M. Nunes, A. S. Adekola, D. W. Bardayan, J. C. Blackmon, K. Y. Chae, K. A. Chipps, J. A. Cizewski, L. Erikson, C. Harlin *et al.*, Phys. Rev. C **84**, 034601 (2011).
[3] R. Kozub, G. Arbanas, A. Adekola, D. Bardayan, J. Blackmon *et al.*, Phys. Rev. Lett. **109**, 172501 (2012).
[4] C. Langer, F. Montes, A. Aprahamian, D. W. Bardayan, D. Bazin, B. A. Brown, J. Browne, H. Crawford, R. H. Cyburt, C. Domingo-Pardo *et al.*, Phys. Rev. Lett. **113**, 032502 (2014).
[5] J. Cizewski *et al.*, J. Phys. Conf. **420**, 012058 (2013).
[6] F. M. Nunes and A. Deltuva, Phys. Rev. C **84**, 034607 (2011).
[7] A. Deltuva and A. C. Fonseca, Phys. Rev. C **79**, 014606 (2009).
[8] N. J. Upadhyay, A. Deltuva, and F. M. Nunes, Phys. Rev. C **85**, 054621 (2012).
[9] A. Deltuva, Phys. Rev. C **88**, 011601 (2013).
[10] A. Lovell and F. Nunes, J. Phys. G **42**, 034014 (2015).
[11] F. D. Becchetti, Jr. and G. W. Greenlees, Phys. Rev. **182**, 1190 (1969).
[12] R. Varner, W. Thompson, T. McAbee, E. Ludwig, and T. Clegg, Phys. Rep. **201**, 57 (1991).
[13] A. Koning and J. Delaroche, Nucl. Phys. A **713**, 231 (2003).
[14] S. P. Weppner, R. B. Penney, G. W. Diffendale, and G. Vittorini, Phys. Rev. C **80**, 034608 (2009).
[15] F. Perey and B. Buck, Nucl. Phys. **32**, 353 (1962).
[16] L. J. Titus and F. M. Nunes, Phys. Rev. C **89**, 034609 (2014).
[17] N. Austern, Phys. Rev. **137**, B752 (1965).
[18] H. Fiedeldey, Nucl. Phys. **77**, 149 (1966).
[19] C. Mahaux and R. Sartor, Adv. Nucl. Phys. **20**, 1 (1991).

[20] J. Mueller, R. Charity, R. Shane, L. Sobotka, S. Waldecker, W. Dickhoff, A. Crowell, J. Esterline, B. Fallin, C. Howell *et al.*, Phys. Rev. C **83**, 064605 (2011).
[21] N. B. Nguyen, S. J. Waldecker, F. M. Nunes, R. J. Charity, and W. H. Dickhoff, Phys. Rev. C **84**, 044611 (2011).
[22] W. H. Dickhoff, D. Van Neck, S. J. Waldecker, R. J. Charity, and L. G. Sobotka, Phys. Rev. C **82**, 054306 (2010).
[23] S. J. Waldecker, C. Barbieri, and W. H. Dickhoff, Phys. Rev. C **84**, 034616 (2011).
[24] H. Dussan, S. J. Waldecker, W. H. Dickhoff, H. Müther, and A. Polls, Phys. Rev. C **84**, 044319 (2011).
[25] M. H. Mahzoon, R. J. Charity, W. H. Dickhoff, H. Dussan, and S. J. Waldecker, Phys. Rev. Lett. **112**, 162503 (2014).
[26] H. Dussan, M. H. Mahzoon, R. J. Charity, W. H. Dickhoff, and A. Polls, Phys. Rev. C **90**, 061603 (2014).
[27] D. Rohe, C. S. Armstrong, R. Asaturyan, O. K. Baker, S. Bueltmann, C. Carasco, D. Day, R. Ent, H. C. Fenker, K. Garrow *et al.*, Phys. Rev. Lett. **93**, 182501 (2004).
[28] J. Dicello, G. Igo, W. Leland, and F. Perey, Phys. Rev. C **4**, 1130 (1971).
[29] H. Ohnuma, J. Kasagi, F. Kakimoto, S. Kubono, and K. Koyama, J. Phys. Soc. Jpn. **48**, 1812 (1980).
[30] R. V. Reid, Jr., Ann. Phys. **50**, 411 (1968).
[31] W. W. Daehnick, J. D. Childs, and Z. Vrcelj, Phys. Rev. C **21**, 2253 (1980).
[32] I. J. Thompson, Comput. Phys. Rep. **7**, 167 (1988).
[33] N. K. Timofeyuk and R. C. Johnson, Phys. Rev. Lett. **110**, 112501 (2013).
[34] N. K. Timofeyuk and R. C. Johnson, Phys. Rev. C **87**, 064610 (2013).